PRP Pharmacology Research & Perspectives
Open Access

ORIGINAL ARTICLE

Downregulation of the Ca^{2+}-activated K^+ channel $K_{Ca}3.1$ by histone deacetylase inhibition in human breast cancer cells

Susumu Ohya[1], Saki Kanatsuka[1], Noriyuki Hatano[2], Hiroaki Kito[1], Azusa Matsui[1], Mayu Fujimoto[1], Sayo Matsuba[1], Satomi Niwa[1], Peng Zhan[3], Takayoshi Suzuki[3] & Katsuhiko Muraki[2]

[1]Department of Pharmacology, Division of Pathological Sciences, Kyoto Pharmaceutical University, Kyoto 607-8414, Japan
[2]Laboratory of Cellular Pharmacology, School of Pharmacy, Aichi-Gakuin University, Nagoya 464-8650, Japan
[3]Graduate School of Medical Science, Kyoto Prefectural University of Medicine, Kyoto 606-0823, Japan

Keywords
Breast cancer, Ca^{2+}-activated K^+ channel, histone deacetylase inhibitor, vorinostat

Correspondence
Susumu Ohya, Department of Pharmacology, Division of Pathological Sciences, Kyoto Pharmaceutical University, 5 Misasagi-Nakauchi, Yamashina, Kyoto 607-8414, Japan. Tel/Fax: +81-75-595-4667;
E-mail: sohya@mb.kyoto-phu.ac.jp

Funding Information
This work was supported by a Grant-in Aid for Scientific Research (C) [No. 25460111] by the Japan Society for the Promotion of Science (JSPS), a research grant from The Promotion and Mutual Aid Cooperation for Private Schools of Japan (Kyoto Pharmaceutical Univ. and Aichi-Gakuin Univ.), a research grant from Supported Program for the Strategic Research Foundation at Private Universities, 2013-2017 from the Ministry of Education, Culture, Sports, Science and Technology (MEXT), Mochida Memorial Foundation for Medical and Pharmaceutical Research, Uehara Memorial Foundation, and Salt Science Research Foundation [No. 1531] (S.O.).

Received: 5 February 2016; Accepted: 12 February 2016

Pharma Res Per, 4(2), 2016, e00225, doi: 10.1002/prp2.228

doi: 10.1002/prp2.228

Abstract

The intermediate-conductance Ca^{2+}-activated K^+ channel $K_{Ca}3.1$ is involved in the promotion of tumor growth and metastasis, and is a potential therapeutic target and biomarker for cancer. Histone deacetylase inhibitors (HDACis) have considerable potential for cancer therapy, however, the effects of HDACis on ion channel expression have not yet been investigated in detail. The results of this study showed a significant decrease in $K_{Ca}3.1$ transcription by HDAC inhibition in the human breast cancer cell line YMB-1, which functionally expresses $K_{Ca}3.1$. A treatment with the clinically available, class I, II, and IV HDAC inhibitor, vorinostat significantly downregulated $K_{Ca}3.1$ transcription in a concentration-dependent manner, and the plasmalemmal expression of the $K_{Ca}3.1$ protein and its functional activity were correspondingly decreased. Pharmacological and siRNA-based HDAC inhibition both revealed the involvement of HDAC2 and HDAC3 in $K_{Ca}3.1$ transcription through the same mechanism. The downregulation of $K_{Ca}3.1$ in YMB-1 was not due to the upregulation of the repressor element-1 silencing transcription factor, REST and the insulin-like growth factor-binding protein 5, IGFBP5. The significant decrease in $K_{Ca}3.1$ transcription by HDAC inhibition was also observed in the $K_{Ca}3.1$-expressing human prostate cancer cell line, PC-3. These results suggest that vorinostat and the selective HDACis for HDAC2 and/or HDAC3 are effective drug candidates for $K_{Ca}3.1$-overexpressing cancers.

Abbreviations

AATB, 4-(acetylamino)-*N*-[2-amino-5-(2-thienyl)phenyl]-benzamide; BCA, breast cancer; DCEBIO, 5,6-dichloro-1-ethyl-1,3-dihydro-2H-benzimidazol-2-one; $DiBAC_4$ (3), bis-(1,3-dibutylbarbituric acid)trimethine oxonol; NDPK, nucleoside diphosphate kinase; EGFR, epidermal growth factor receptor; ER, estrogen receptor; FCM, flow cytometry; HDAC, histone deacetylase; HDACi, HDAC inhibitor; HER, epidermal growth factor receptor; HNSCC, head and neck squamous cell carcinoma; ICA-17043, 2,2-bis(4-fluorophenyl)-2-phenyl-acetamide; K_{Ca}, Ca^{2+}-activated K^+ (channel); MTMR, myotubularin-related protein; NDPK, nucleoside diphosphate kinase; PHPT, phosphohistidine phosphatase; PI3K-C2B, phosphoinositide-3-kinase, class 2, β polypeptide; PR, progesterone receptor; PRL, prolactin; REST, repressor element 1-silencing transcription factor; siRNA, small interfering RNA; SIRT, sirtuin; T247, *N*-(2-aminophenyl)-4-[1-(2-thiophen-3-ylethyl)-1H-[1], [2], [3]triazol-4-yl]benzamide; NCT-14b, (S)-S-7-(adamant-1-ylamino)-6-(tert-butoxycarbonyl)-7-oxoheptyl-2-methylpropanethioate; TRAM-34, 1-[(2-chlorophenyl) diphenylmethyl]-1H-pyrazole; *WST-1*, 2-(4-Iodophenyl)-3-(4-nitrophenyl)-5-(2,4-disulfophenyl)-2H-tetrazolium, monosodium salt.

Introduction

The Ca^{2+}-activated K^+ (K_{Ca}) channel contributes to the feedback mechanism required to enhance Ca^{2+} signaling by controlling Ca^{2+} entry through Ca^{2+} release-activated Ca^{2+} channels in nonexcitable cells such as cancer and immune cells (Cahalan and Chandy 2009; Bergmeier et al. 2013; Huang and Jan 2014; Pardo and Stühmer 2014; Comes et al. 2015; Feske et al. 2015). Based on the single-channel conductance, K_{Ca} channels have been classified into large conductance ($K_{Ca}1.1$), intermediate conductance ($K_{Ca}3.1$, also known as IK_{Ca}, SK4, and KCNN4), and small conductance ($K_{Ca}2.x$) channels. The blockade of $K_{Ca}3.1$ inhibits proliferation and invasion during metastasis and/or promotes apoptosis in several cancer types including breast cancer (Wulff and Castle 2010; Ouadid-Ahidouch and Ahidouch 2013). Breast cancer is the most commonly occurring malignancy among women, and $K_{Ca}3.1$ has been identified as one of the new loci associated with susceptibility to breast cancer by large-scale genotyping analyses (Michailidou et al. 2013). Since $K_{Ca}3.1$ increased with the progression of breast cancer, it may be useful as a tumor marker to detect the malignancy grade during breast cancer progression (Haren et al. 2010). The luteotropic hormone, prolactin (PRL) has been associated with an increased risk of breast cancer, and PRL-induced $K_{Ca}3.1$ activation promotes the proliferation of breast cancer cells (Faouzi et al. 2010). Of the four $K_{Ca}3.1$ regulators identified to date (class II phosphatidylinositol 3 kinase C2β (PI3K-C2B), nucleoside diphosphate kinase-B (NDPK-B), protein histidine phosphatase 1 (PHPT1), and phosphatidylinositol 3-phosphate phosphatase myotubularin-related protein 6 (MTMR6), NDPK-B is involved in various cellular functions in cancer cells and is a potential therapeutic target for breast cancer (Attwood and Wieland 2015).

Histone deacetylase inhibitors (HDACis), which exhibit a broad spectrum of epigenetic activities, are emerging as anticancer drugs (Bose et al. 2014). The suberoylanilide hydroxamic acid vorinostat received FDA approval for the treatment of cutaneous T-cell lymphoma and is a pan-HDACi that inhibits class I, II, and IV HDAC subtypes. HDACis are a novel class of agents in the treatment of solid cancers (Slingerland et al. 2014), and several clinical studies have been conducted on vorinostat as a combination therapy (Munster et al. 2011; Ramaswamy et al. 2012). HDACis reverse DNA methylation in cancer cells, and have clinical activity in the treatment of cancers (West and Johnstone 2014). We previously reported that the transcription of the Ca^{2+}-activated Cl^- channel TMEM16A is downregulated by vorinostat and the pharmacological and small interfering RNA
(siRNA)-based blockade of HDAC3 (Matsuba et al. 2014); however, the regulation of other ion channels by HDAC inhibition remains to be elucidated. The destabilization of DNA methylation (hypermethylation or hypomethylation) in ion channels has been correlated with tumorigenesis and a poor prognosis (Ouadid-Ahidouch et al. 2015). Hypomethylation of the $K_{Ca}3.1$ promoter has recently been associated with the upregulation of $K_{Ca}3.1$ in lung cancer cells (Bulk et al. 2015).

We herein demonstrated that the expression of $K_{Ca}3.1$ was downregulated in the human breast cancer cell line YMB-1 by treatment with the pan-HDAC inhibitor vorinostat. Pharmacological and siRNA-based HDAC inhibition experiments indicated that $K_{Ca}3.1$ transcription is regulated by HDAC2 and HDAC3 through the same mechanism. Taken together, these results suggest that vorinostat and HDAC2/3-selective inhibitors are effective against $K_{Ca}3.1$-overexpressing cancers and other $K_{Ca}3.1$-overexpressing disorders such as autoimmune and inflammatory diseases.

Materials and Methods

Cell culture and cell viability assay

The breast cancer cell lines MDA-MB-453, YMB-1, MCF-7, Hs578T-Luc, and BT-549 and the prostate cancer cell lines PC-3 and LNCaP (clone FGC) were supplied by the RIKEN BioResource Center (RIKEN BRC) (Tsukuba, Japan) and Health Science Research Resources Bank (HSRRB) (Osaka, Japan). They were maintained at 37°C, in 5% CO_2 with RPMI 1640, Dulbecco's modified Eagle's (DMEM), or Leibovitz's L-15 medium (Wako, Osaka, Japan) containing 10% fetal bovine serum (Sigma, St. Louis, MO) and a penicillin (100 units/mL)-streptomycin (0.1 mg/mL) mixture (Wako) (Matsuba et al. 2014). A cell viability assay *using WST-1* was performed as described in our previous study (Matsuba et al. 2014). Briefly, using a density of 4×10^5 cells/mL, cells were cultured in duplicate on 96-well plates for 48 h (Fig. 1D) or 72 h (Fig. 1C, E). Absorbance was measured 2 h after the addition of WST-1 reagent into each well using the microplate reader MULTSCAN FC (Thermo Fisher Scientific, Yokohama, Japan) at a test wavelength of 450 nm and reference wavelength of 620 nm. A pair of control and treated samples was prepared from different passage cells, and then the same protocol was repeated on another day. Cell viability of the vehicle (0.1% dimethyl sulfoxide)-treated cells was arbitrarily expressed as 1.0.

Transfecting cells with siRNA

Lipofectamine RNAiMAX reagent was used for all siRNA transfection procedures (Matsuba et al. 2014). Commer-

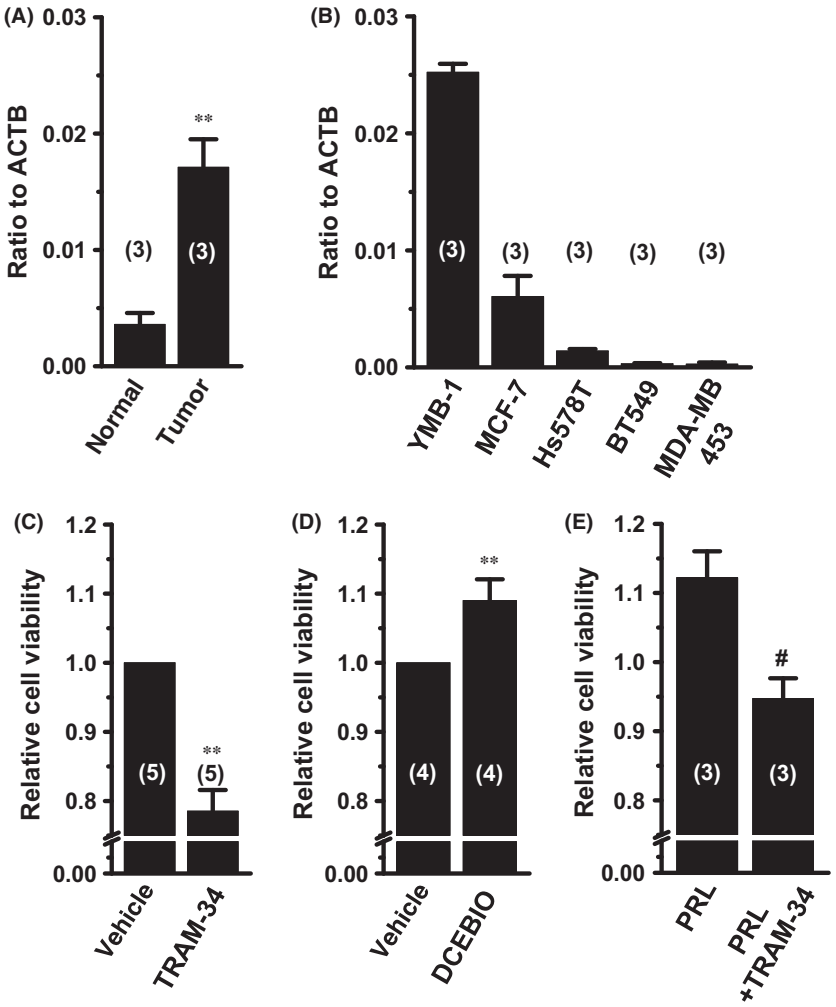

Figure 1. Expression levels of $K_{Ca}3.1$ transcripts in human breast tumors and breast cancer cell lines and effects of $K_{Ca}3.1$ blockade on cell proliferation in YMB-1 cells. (A and B) Real-time PCR assay for $K_{Ca}3.1$ in normal and tumor breast tissues (A) and human breast cancer cell lines (YMB-1, MCF-7, Hs578T, BT549 and MDA-MB-453). (C) Effects of the selective $K_{Ca}3.1$ blocker, TRAM-34 (1 and 10 μmol/L) on cell viability in YMB-1 cells. (D) Effects of the $K_{Ca}3.1$ activator, 10 μmol/L DCEBIO on cell viability in YMB-1 cells. (E) Effect of 1 μmol/L TRAM-34 on cell viability in YMB-1 cells pretreated with PRL (200 nmol/L). In (A and B) the expression levels of $K_{Ca}3.1$ transcripts are expressed as $K_{Ca}3.1/\beta$-actin (ACTB) ratio. In (C, D, and E) the cell viability in vehicle control (without treatment with PRL and TRAM-34) was expressed as 1.0. Results are expressed as means ± SEM. The numbers used for the experiments are shown in parentheses. The significance of differences was evaluated using the Student's *t*-test. $^{**}P < 0.01$ versus normal tissues and vehicle control. $^{\#}P < 0.05$ versus PRL.

cially available siRNA oligonucleotides against $K_{Ca}3.1$ (sc-91691), HDAC2 (sc-29345), HDAC3 (sc-35538), and control siRNA (type A) were purchased from Santa Cruz Biotechnology (Santa Cruz, CA). The expression levels of the target transcripts were assessed 48 h after transfection of siRNAs using a real-time PCR assay, and cell viability was measured by the WST-1 assay.

RNA extraction, reverse transcription, and real-time PCR

Total RNAs from normal human and tumor tissues were purchased from TaKaRa BIO (Osaka, Japan), BD Biosciences (San Jose, CA), and BioChain (Hayward, CA). Total RNAs from the primary tumor and corresponding metastatic tumor of the same donor (a 65-year-old female) were purchased from BioChain, who confirmed the expression of tumor-specific genes and tumor metastatic genes, respectively, in these tumors. Total RNA extraction from cell lines and reverse transcription were performed as previously reported (Matsuba et al. 2014). cDNA products were amplified with gene-specific PCR primers, designated using Primer Express™ software (Ver 3.0.1; Life Technologies, Carlsbad, CA). Quantitative, real-time PCR was performed using SYBR Green chemistry on an ABI 7500 sequence detector system (Thermo-

Fisher Scientific). The following gene-specific PCR primers of human origin were used for real-time PCR: $K_{Ca}3.1$ (GenBank accession number: NM_002250, 1475-1595), amplicon = 121 bp; NDPK-B (NM_002512, 288-408), 121 bp; repressor element 1-silencing transcription factor (REST) (NM_005612, 1415-1545), 131 bp; insulin-like growth factor 5 (IGFBP5) (NM_000599, 1088-1208), 121 bp; histone deacetylase (HDAC) 2 (NM_001527, 298-405), 108 bp; HDAC3 (NM_003883, 699-819), 121 bp; β-actin (ACTB) (NM_001101, 411-511), 101 bp. Unknown quantities relative to the standard curve for a particular set of primers were calculated as previously reported (Matsuba et al. 2014), yielding the transcriptional quantitation of gene products relative to the endogenous standard, ACTB.

Overexpression of IGFBP5 in YMB-1 cells

The cDNA products from YMB-1 cells were amplified with KOD FX DNA polymerase (TOYOBO, Osaka, Japan) and PCR primers specific for human IGFBP5: IGFBP5 (NM_000599, 717-1629), 913 bp. The amplification profile was follows: a 2 min predenaturation step at 94°C, followed by 40 cycles of a 10 sec denaturation step at 98°C and a 1 min primer extension step at 68°C for 40 cycles. Obtained amplified products of full-length IGFBP5 were ligated into pcDNA3.1(+)/Neo^r (Invitrogen) (pcDNA-IGFBP5). The nucleotide sequences of plasmid constructs were determined by Eurofins Genomics (Tokyo, Japan). YMB-1 cells were transiently transfected with pcDNA-IGFBP5 using Lipofectamine 2000 (Invitrogen). Forty-eight hours after transfection, the expression levels of IGFBP5 and $K_{Ca}3.1$ transcripts were determined by real-time PCR assay.

Protein expression analyses by Western blotting and immunocytochemistry

Proteins lysates were prepared from YMB-1 cells for Western blot analysis, as previously reported (Matsuba et al. 2014). Protein expression levels were determined 48 h after the compound treatment. Equal amounts of protein (20 μg/lane) were subjected to SDS-PAGE (10%). Blots were incubated with anti-$K_{Ca}3.1$ (Alomone Labs, Jerusalem, Israel) and anti-ACTB (Medical & Biological Laboratories (MBL), Nagoya, Japan) antibodies, then incubated with anti-rabbit and anti-mouse horseradish peroxidase-conjugated IgG (Merck Millipore, Darmstadt, Germany), respectively. An enhanced chemiluminescence detection system (GE Healthcare Japan, Tokyo, Japan) was used to detect the bound antibody. The resulting images were analyzed by a VersaDoc5000MP device (Bio-Rad Laboratories, Hercules, CA). In the immunocytochemical examination, living YMB-1 cells were harvested using a sterile cell scraper, and stained by an ATTO 488-conjugated anti-$K_{Ca}3.1$ (extracellular) antibody for live cell imaging (Alomone Labs). Stained cells were subjected to an analysis on a FACSCalibur flow cytometer using CellQuest software (BD Biosciences).

Measurements of $K_{Ca}3.1$ K^+ currents by whole-cell patch-clamp recordings

Whole-cell patch-clamp experiments were performed as reported previously (Matsuba et al. 2014). A pipette solution was used, with the following composition (in mmol/L): 110 K-aspartate, 30 KCl, 1 $MgCl_2$, 10 HEPES, 10 EGTA, and 2 Na_2ATP (pH 7.2 by KOH). Ca^{2+} concentrations (pCa 6.5) were determined using the WINMAXC program (Stanford University, Stanford, CA). Membrane currents were digitized using an analog-digital converter (PCI6229, National Instruments, Tokyo, Japan), and data acquisition and analysis were performed using WinWCP4.65, developed by Dr. John Dempster (University of Strathclyde, UK). The liquid junction potential between the pipette and bath solutions (−10 mV) was corrected. Cells were held at −80 mV and currents were evoked by pipette solutions containing Ca^{2+} buffered at 300 nmol/L. Outward K^+ currents were determined by stepping the cell from −80 to +40 mV for 100 msec, and then to −40 mV to measure the tail current (see Fig. S3A). A standard HEPES-buffered bathing solution was used, with the following composition (in mmol/L): 137 NaCl, 5.9 KCl, 2.2 $CaCl_2$, 1.2 $MgCl_2$, 14 glucose, and 10 HEPES (pH 7.4 by NaOH). All experiments were performed at 25 ± 1°C.

Measurement of the intracellular Ca^{2+} concentrations by the fluorescent Ca^{2+} indicator dye

Cells were seeded onto 35 mm glass bottom dishes and cultured at 37°C in 5% CO_2 humidified incubator. Intracellular Ca^{2+} concentration was measured using the fluorescent Ca^{2+} indicator dye, Fura 2-AM. Cells were incubated with 10 μmol/L Fura 2-AM in normal HEPES solution for 30 min at room temperature. Cells loaded with Fura 2-AM were alternatively illuminated at wavelengths of 340 and 380 nm, and fluorescence images were recorded on the ORCA-Flash2.8 digital camera (Hamamatsu Photonics, Hamamatsu, Japan). Data collection and analyses were performed using an HCImage system (Hamamatsu Photonics). Images were measured every 5 sec. The fluorescent intensity of Fura 2 was expressed as measured 340/380 nm fluorescence ratios [ratio (340/380)] after background subtraction. After treatment with a sarco/endoplasmic reticulum Ca^{2+}-

ATPase (SERCA) inhibitor, thapsigargin (1 μmol/L) under 0 mmol/L Ca^{2+} in a bathing medium, application of 2.2 mmol/L Ca^{2+} caused store-operated Ca^{2+} entry (SOCE) (see Fig. S3B). Ten minutes after 1st application of 2.2 mmol/L Ca^{2+}, second one was performed in the presence of 1 mmol/L TRAM-34. The value of area under the curve (AUC) of the ratio (340/380) was obtained by the integration on the computer. The AUC value in the second application was normalized by that of the first one (relative AUC of $[Ca^{2+}]_i$).

Chemicals

The sources of pharmacological agents were as follows: TRAM-34 (Santa Cruz Biotechnology), ICA-17043 (Cheminstock Ltd., Shanghai, China), $DiBAC_4(3)$ (Invitrogen), DCEBIO (TOCRIS Bioscience, Ellisville, MO), paclitaxel (Sigma-Aldrich, St. Louis, MO, USA), PRL (Wako), *WST-1* (Dojindo, Kumamoto, Japan), and Fura2-AM (Dojindo). HDAC inhibitors (vorinostat, AATB, T247, NCT-14b and NCO-04) were supplied by Professor Suzuki (KPUM). Others were obtained from Sigma-Aldrich or Wako Pure Chemical Industries (Tokyo, Japan).

Statistical analysis

The significance of differences among two and multiple groups was evaluated using the Student's *t*-test and Tukey's test after the *F*-test or ANOVA, respectively. Significance at $P < 0.05$ and $P < 0.01$ is indicated in the figures. Data are presented as the means $\pm$ SEM.

Results

High level expression of the $K_{Ca}3.1$ K^+ channel in breast tumor tissues and the breast cancer cell line, YMB-1

Figure 1A shows that $K_{Ca}3.1$ transcripts were more strongly expressed in human breast tumor tissues than in normal breast tissues. Of the five human breast cancer cell lines examined, the high level expression of $K_{Ca}3.1$ transcripts was detected in YMB-1 cells (Fig. 1B). YMB-1 and MDA-MB-453 cells were human epidermal growth factor receptor 2 (HER2)-positive; however, no correlation was found between $K_{Ca}3.1$ and HER2. We next examined the effects of the selective $K_{Ca}3.1$ blocker, TRAM-34 and $K_{Ca}2.x$ and $K_{Ca}3.1$ activator, DCEBIO on the viability of YMB-1 cells. Cell viability significantly decreased in YMB-1 cells treated for 72 h with 10 μmol/L TRAM-34 (Fig. 1C), and significantly increased in those treated with 1 μmol/L DCEBIO (Fig. 1D). Faouzi et al. (2010) have shown that $K_{Ca}3.1$ activity is significantly enhanced by a treatment with PRL and PRL-induced proliferation is inhibited by the pharmacological blockade of $K_{Ca}3.1$. In this study, PRL receptor (PRLR) transcripts were strongly expressed in YMB-1 cells (Fig. S1A). As shown in Figure 1E, the enhancement induced in cell viability by the treatment with 200 nmol/L PRL for 72 h was significantly decreased by that with TRAM-34 (10 μmol/L). Of 51 K^+ channel subtypes (28 voltage-gated Kv subtypes, 15 two-pore domain K_{2P} subtypes, 7 Ca^{2+}-activated K_{Ca} subtypes, and inward-rectifier $K_{ir}2.1$), YMB-1 cells predominantly expressed $K_{Ca}3.1$ transcripts (Fig. S2A–F), and no significant decrease in cell viability were detected in YMB-1 cells treated for 48 h with 10 mmol/L tetraethylammonium (TEA) (a Kv inhibitor) and 1 mmol/L Ba^{2+} (a K_{2P} inhibitor) (Fig. S2G).

Downregulation of $K_{Ca}3.1$ gene and protein expression in YMB-1 cells by the treatment with vorinostat

As shown in our previous study (Matsuba et al. 2014), vorinostat (1 and 10 μmol/L) significantly inhibits the viability of YMB-1 cells in a concentration-dependent manner. Real-time PCR examinations revealed that the treatment of YMB-1 cells with vorinostat for 24 h significantly downregulated the expression levels of the $K_{Ca}3.1$ transcripts in a concentration-dependent manner ($n = 4$, $P < 0.05$ and 0.01 vs. vehicle control) (Fig. 2A). Similarly, the expression levels of the $K_{Ca}3.1$ proteins in YMB-1 cells were suppressed by the treatment with vorinostat for 48 h in a concentration-dependent manner (Fig. 2B). Similar results were obtained from three independent experiments. The optical density of the $K_{Ca}3.1$ protein band signal relative to that of the ACTB one was calculated by ImageJ software (Ver. 1.42, NIH, Bethesda, MD), and protein expression levels in the vehicle control were then expressed as 1.00. Relative optical densities in vorinostat-treated groups (1 and 10 μmol/L) were 0.80 ± 0.04 ($n = 3$, $P < 0.05$) and 0.59 ± 0.05 ($n = 3$, $P < 0.01$). We also measured the protein expression levels of $K_{Ca}3.1$ in the plasma membrane with an ATTO 488-conjugated anti-$K_{Ca}3.1$ (extracellular) antibody (Alomone Labs), which has the ability to distinguish the extracellular region of $K_{Ca}3.1$ by a FCM analysis. A decrease in the percentage of $K_{Ca}3.1$-positive cells was observed by the treatment with 1 μmol/L vorinostat for 48 h (Fig. 2C and D). In MDA-MB-453 cells weakly expressing $K_{Ca}3.1$, the percentage of ATTO 488-positive cells was less than 3% (not shown). The chemotherapy drugs paclitaxel (100 nmol/L) and bafilomycin-A (10 nmol/L, a vacuolar-ATPase inhibitor) markedly suppressed cell proliferation in these cell lines, whereas no suppressive effects were observed on $K_{Ca}3.1$ transcription (Fig. S1B). Additionally, the inhibition of SIRT1 and 2 (class III HDAC subtypes) by NCO-04 (50 μmol/L)

(Suzuki et al., 2012) did not significantly downregulate the expression of $K_{Ca}3.1$ in YMB-1 cells (Fig. S1C and D).

Decrease in $K_{Ca}3.1$ activities in YMB-1 cells by the treatment with vorinostat

Outward K^+ currents were recorded by the application of depolarizing steps (from −80 to +40 mV for 100 msec) using the whole-cell configuration. Tail currents were then measured at −40 mV after depolarization to +40 mV for 100 msec. $K_{Ca}3.1$ K^+ currents were estimated as 1 μmol/L TRAM-34-sentitive components. Both peak and tail $K_{Ca}3.1$ K^+ currents sensitive to TRAM-34 were significantly smaller in 10 μmol/L vorinostat-treated than in vehicle-treated YMB-1 cells (Fig. 3). Both peak (Fig. 3A) and tail (Fig. 3B) current amplitudes were over

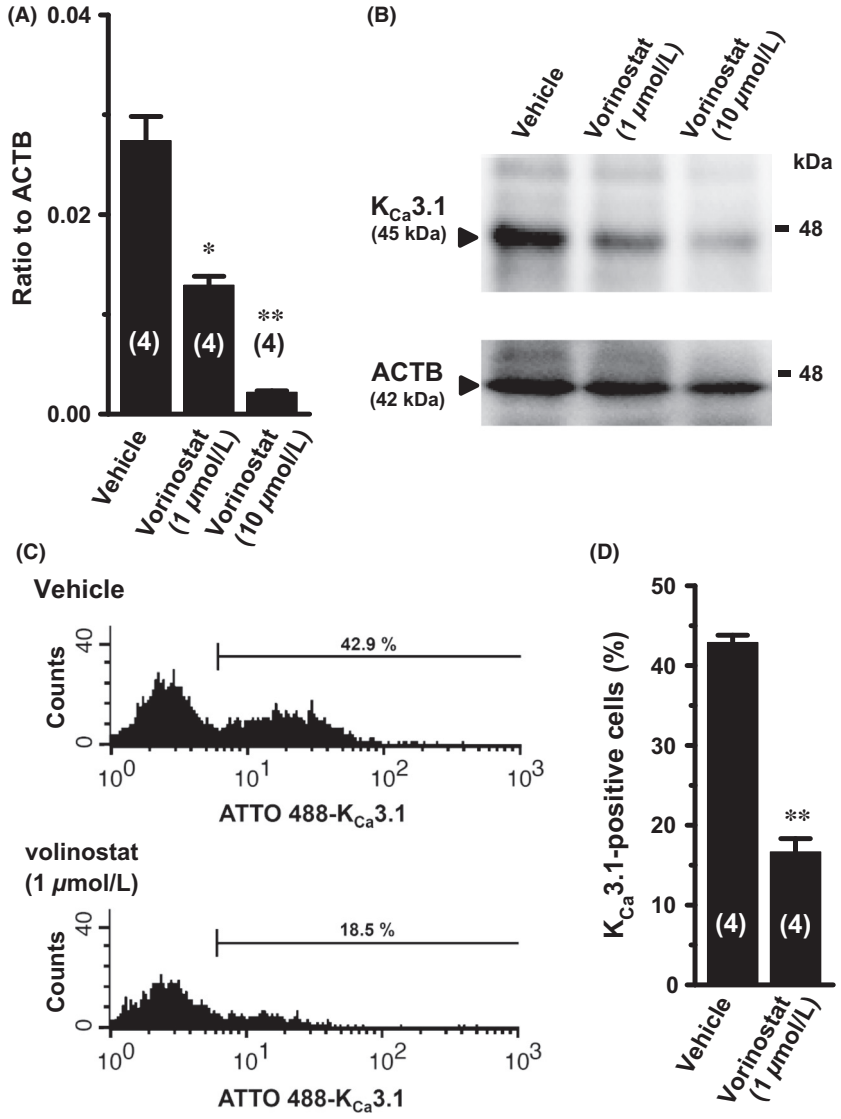

Figure 2. Effects of vorinostat on $K_{Ca}3.1$ gene and protein expression levels in YMB-1 cells. (A) Effects of vorinostat (1 and 10 μmol/L) on the expression levels of $K_{Ca}3.1$ transcripts. Expression levels are expressed as $K_{Ca}3.1$/ACTB ratio. (B–D) Effects of vorinostat on the expression levels of $K_{Ca}3.1$ proteins in YMB-1 cells in Western blotting (B) and flow cytometric analyses (C and D). In (B) proteins from the plasma membrane fraction of YMB-1 cells were probed by immunoblotting with anti-$K_{Ca}3.1$ (upper panel) and anti-ACTB (lower panel) antibodies on duplicate filters. Arrowheads indicate the migrating positions of $K_{Ca}3.1$ and ACTB. Molecular mass standards are shown in kDa on the right side of the panels. In (C) living YMB-1 cells were stained with an ATTO 488-fused anti-$K_{Ca}3.1$ (extracellular) antibody, and ATTO 488-positive cells were measured using flow cytometry. Data were expressed as the percentage of $K_{Ca}3.1$-positive cells (D). Results are expressed as means ± SEM. The numbers used for the experiments are shown in parentheses. The significance of differences among two and multiple groups was evaluated using the Student's *t*-test and Tukey's test. *,**$P < 0.05$, 0.01 versus vehicle control.

80% decreased in vorinostat-treated YMB-1 cells. Next, we examined the effects of TRAM-34 on the SOCE in vehicle- and 10 μmol/L vorinostat-treated YMB-1 cells. In vehicle-treated YMB-1 cells, significant decrease in relative AUC of $[Ca^{2+}]_i$ due to membrane depolarization elicited by $K_{Ca}3.1$ inhibition was observed (Fig. 3C), whereas it was disappeared in vorinostat-treated YMB-1 cells (Fig. 3D). TRAM-34-induced decrease in the relative peak amplitude of transient Ca^{2+} rise (peak 2/peak 1, see Fig. S3A) was also disappeared by the treatment with 10 μmol/L vorinostat (not shown).

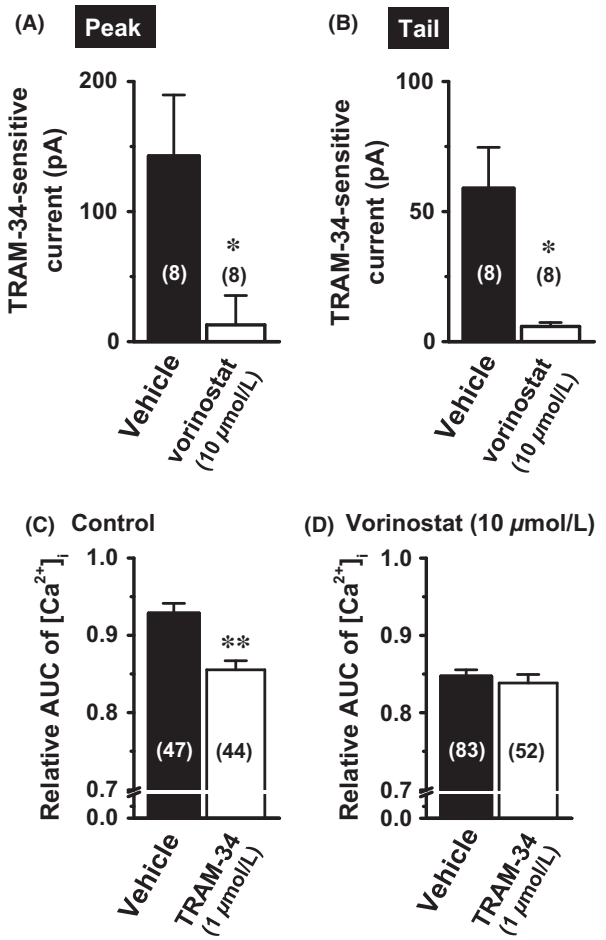

Figure 3. Inhibition of $K_{Ca}3.1$ activity in YMB-1 cells by the treatment with vorinostat. Pharmacological experiments using 1 μmol/L TRAM-34 were performed using whole-cell patch-clamp recording and Ca^{2+} imaging systems. (A and B) TRAM-34 (1 μmol/L)-sensitive outward peak (A) and tail (B) currents at +40 mV in vehicle- and 10 μmol/L vorinostat-treated YMB-1 cells for 30–48 h. (C and D) TRAM-34 (1 μmol/L)-induced changes in store-operated Ca^{2+} entry in vehicle- (control) (C) and 10 μmol/L vorinostat-treated (D) YMB-1 cells for 30–48 h. Relative AUC of $[Ca^{2+}]_i$ was calculated as described in "Materials and Methods." Results are expressed as means ± SEM. Numbers used for the experiments are shown in parentheses. The significance of differences was evaluated using the Student's *t*-test. *, **$P < 0.05$, 0.01 versus vehicle control.

Identification of HDAC subtypes involved in the downregulation of $K_{Ca}3.1$ in YMB-1 cells by pharmacological and siRNA-based blockade of HDACs

The HDAC1, HDAC2, HDAC3, and HDAC6 subtypes are predominantly expressed in YMB-1 cells and human tumor breast tissues (Müller et al. 2013; Matsuba et al. 2014; Seo et al. 2014). In order to identify the HDAC subtypes involved in the downregulation of $K_{Ca}3.1$ in YMB-1 cells, the following selective HDAC inhibitors were used: 30 nmol/L AATB, 300 nmol/L AATB, 1 μmol/L T247, and 1 μmol/L NCT-14b for the selective inhibition of HDAC1, HDAC1/2, HDAC3, and HDAC6, respectively (Itoh et al. 2007; Methot et al. 2008; Suzuki et al. 2013). As shown in Figure 4A, the transcription of $K_{Ca}3.1$ was significantly decreased by the treatment with 300 nmol/L AATB or 1 μmol/L T247 (for 48 h). The treatment with 300 nmol/L AATB plus 1 μmol/L T247 did not exhibit additive or synergistic inhibitory effects on $K_{Ca}3.1$ transcription (Fig. 4A). The treatments with 30 nmol/L AATB and 1 μmol/L NCT-14b did not elicit any significant changes in $K_{Ca}3.1$ transcription. Similarly, the cell surface protein expression of $K_{Ca}3.1$ was significantly suppressed by the treatment with 300 nmol/L AATB or 1 μmol/L T247 (Fig. 4B). In consistent with these results, decrease in relative AUC of $[Ca^{2+}]_i$ elicited by $K_{Ca}3.1$ inhibition was prevented in AATB (300 nmol/L)- and T247 (1 μmol/L)-treated YMB-1 cells (Fig. S3C and D). We further examined the siRNA-based inhibition of HDAC subtypes. We first determined transfection conditions with more than 90% cell viability efficacy using Lipofectamine RNAiMAX. In YMB-1 cells, transfection efficacy was 50–60% under this optimum condition. HDAC2 or HDAC3 were 50% inhibited by HDAC2 or HDAC3 siRNAs (Fig. 5A and B). Similar to the results shown in Figure 4, $K_{Ca}3.1$ transcripts were downregulated by HDAC2 or HDAC3 siRNA (Fig. 5C). The transcription of $K_{Ca}3.1$ was suppressed to a similar level by the transfection of $K_{Ca}3.1$ siRNA (Fig. 5C). These results suggest that the inhibition of HDAC2 or HDAC3 may cause the downregulation of $K_{Ca}3.1$ in YMB-1 cells through the same mechanism. The expression levels of $K_{Ca}3.1$ transcripts were higher in the androgen-independent prostate cancer cell line PC-3 than in the androgen-dependent prostate cancer cell line LNCaP: 0.047 ± 0.002 and less than 0.0002 in arbitrary units, respectively. The downregulation of $K_{Ca}3.1$ by the treatment with vorinostat (Fig. 6A) and HDAC2 or HDAC3 inhibition (Fig. 6B) was also detected in PC-3 cells.

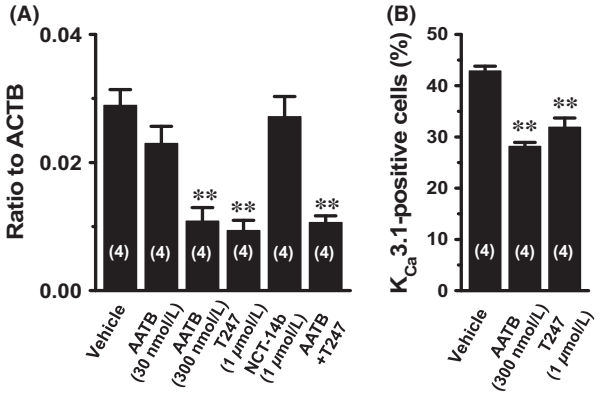

Figure 4. Effects of selective HDAC inhibitors on $K_{Ca}3.1$ gene and protein expression levels in YMB-1 cells. (A) Effects of AATB (30 nmol/L, selective for HDAC1; 300 nmol/L, selective for HDAC1 and 2), T247 (1 μmol/L, selective for HDAC3), NCT-14b (1 μmol/L, selective for HDAC6) and AATB (300 nmol/L) plus T247 (1 μmol/L) on the expression levels of $K_{Ca}3.1$ transcripts in YMB-1 cells. Expression levels were expressed as $K_{Ca}3.1$/ACTB ratio. (B) Effects of AATB (300 nmol/L), T247 (1 μmol/L), and AATB (300 nmol/L) plus T247 (1 μmol/L) on the cell surface expression of $K_{Ca}3.1$ proteins by flow cytometric analysis. Living YMB-1 cells were stained with an ATTO 488-fused anti-$K_{Ca}3.1$ (extracellular) antibody and ATTO 488-positive cells were measured by flow cytometry. Data were expressed as the percentage of $K_{Ca}3.1$-positive cells. Results are expressed as means ± SEM. The numbers used for the experiments are shown in parentheses. The significance of differences was evaluated using the Tukey's test. $^{**}P < 0.01$ versus vehicle control.

Effects of HDACis on the expression of $K_{Ca}3.1$ regulators in YMB-1 cells

Nucleotide diphosphate kinase (NDPK)-B is strongly expressed in many cancer types and, thus, is a potent therapeutic target for anticancer drugs (Attwood and Wieland 2015). In T cells, NDPK-B is a well-known positive regulator of $K_{Ca}3.1$ (Di et al. 2010b; Ohya et al. 2014). As shown in Figure 7A, NDPK-B transcripts were strongly expressed in human breast tumor tissues and YMB-1 cells. The pharmacological and siRNA-based blockade of HDAC2 and HDAC3 did not significantly affect the expression levels of NDPK-B transcripts (Fig. 7B–D). Furthermore, the other positive and negative regulators of $K_{Ca}3.1$, and the transcriptional expression levels of PI3K-C2B, PHPT1, and MTMR6 (Srivastava et al. 2006, 2008, 2009) were not affected by the treatment with 10 μmol/L vorinostat (Fig. S4).

Effects of HDAC inhibition on the expression of REST and IGFBP5 in YMB-1 cells

Repressor element 1-silencing transcription factor, REST (also known as neuron-restrictive silencer factor, NRSF)

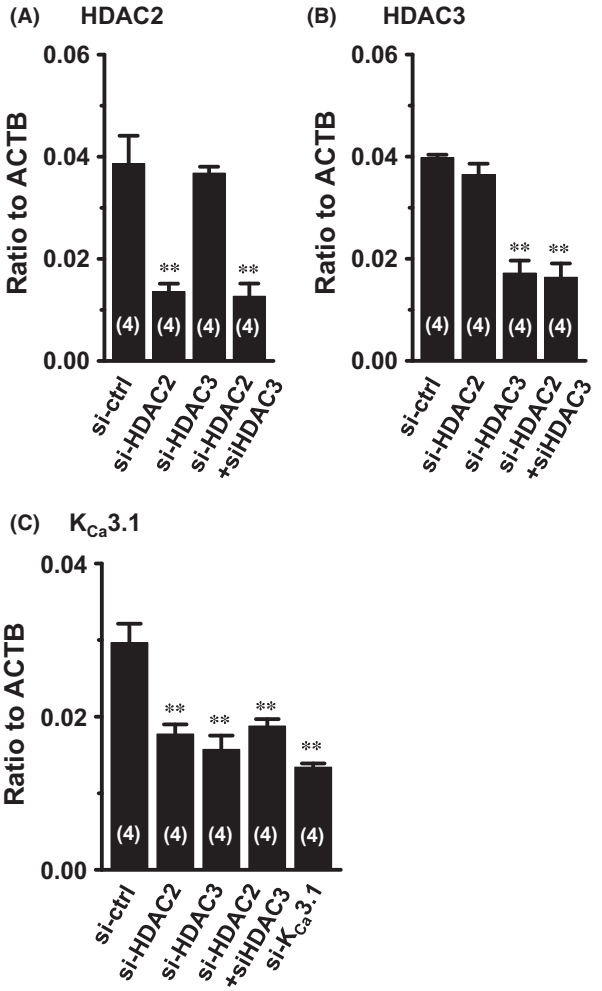

Figure 5. Effects of HDAC2 and HADC3 siRNAs on the expression levels of $K_{Ca}3.1$ transcripts in YMB-1 cells. (A and B) Effects of HDAC2 and/or HDAC3 siRNAs on the expression levels of HDAC2 (A) and HDAC3 (B) transcripts. (C) Effects of HDAC2 and/or HDAC3 siRNAs on the expression levels of $K_{Ca}3.1$ transcripts. Control siRNA-A (Santa Cruz Biotechnology) was used as control siRNA (si-ctrl). Expression levels were expressed as $K_{Ca}3.1$/ACTB ratio. Results are expressed as means ± SEM. The numbers used for the experiments are shown in parentheses. The significance of differences was evaluated using the Tukey's test. $^{**}P < 0.01$ versus control siRNA (si-ctrl).

is known as a transcriptional repressor of $K_{Ca}3.1$ (Cheong et al. 2005; Ohya et al. 2011a), and the transcription or protein degradation of REST is regulated by the treatment with HDACis (Taylor et al. 2012). Therefore, we determined whether the downregulation of $K_{Ca}3.1$ by HDAC inhibition is due to an increase in REST expression in YMB-1 cells. As shown in Figure 8A and B, no significant changes in the transcriptional and protein expression levels of REST were found in vorinostat (1 and 10 μmol/

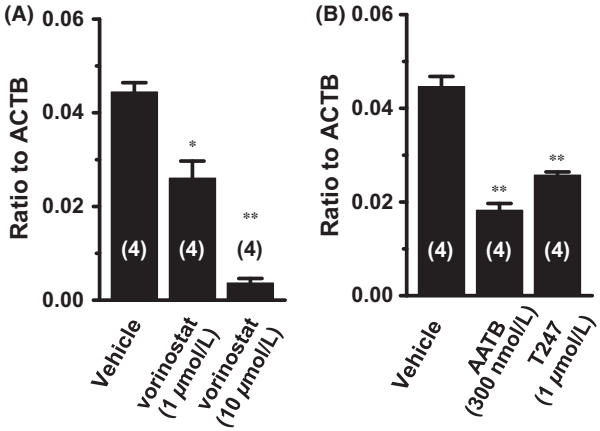

Figure 6. Effects of HDACis on the expression levels of $K_{Ca}3.1$ transcripts in the prostate cancer cell line, PC-3. (A) Effects of 1 and 10 μmol/L vorinostat on the expression levels of $K_{Ca}3.1$ transcripts. (B) Effects of AATB (300 nmol/L) and T247 (1 μmol/L) on the expression levels of $K_{Ca}3.1$ transcripts in PC-3 cells. Expression levels were expressed as $K_{Ca}3.1$/ACTB ratio. The results are expressed as means ± SEM. The numbers used for the experiments are shown in parentheses. The significance of differences was evaluated using the Tukey's test. *,**$P < 0.05$, 0.01 versus vehicle control.

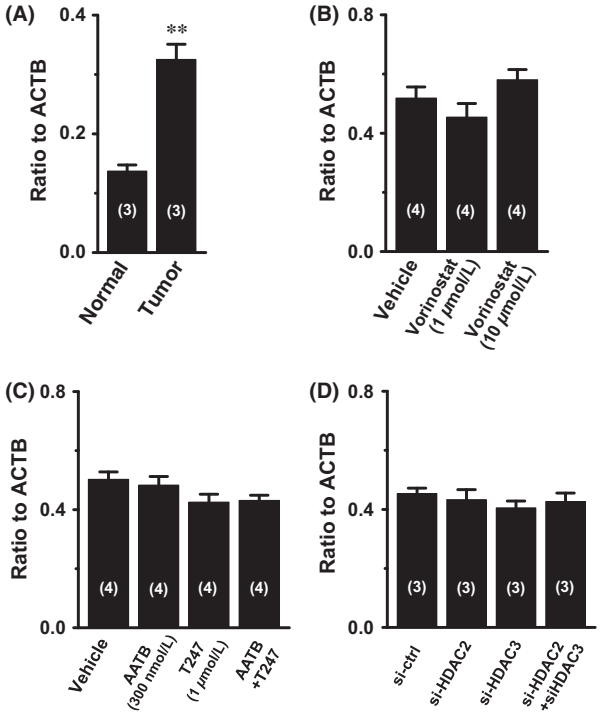

Figure 7. Effects of HDAC inhibitors on the expression levels of NDPK-B transcripts in YMB-1 cells. (A) Expression levels of NDPK-B transcripts in normal and tumor breast tissues. (B–D) Effects of vorinostat (1 and 10 μmol/L) (B), selective HDAC inhibitors (C), and HDAC siRNAs (D) on the expression levels of NDPK-B transcripts in YMB-1 cells. Expression levels were expressed as NDPK-B/ACTB ratio. Results are expressed as means ± SEM. The numbers used for the experiments are shown in parentheses. The significance of differences among two and multiple groups was evaluated using the Student's *t*-test and Tukey's test. **$P < 0.01$ versus normal tissues.

L)-, AATB (300 nmol/L), and T247 (1 μmol/L)-treated YMB-1 cells. When REST transcription was approximately 50% inhibited by the transfection of REST siRNA in YMB-1 cells (not shown), no significant changes in the expression levels of $K_{Ca}3.1$ transcripts were found (Fig. 8C).

It has been reported that insulin-like growth factor-binding protein 5 (IGFBP5) plays an important role in breast cancer progression and metastasis (Wang et al. 2008; Ghoussaini et al. 2014). Recently, Akkiprik et al. (2015) have shown $K_{Ca}3.1$ gene expression is negatively correlated with IGFBP5 one in breast cancer tissues. Using total RNAs from the primary breast tumor and corresponding metastatic breast tumor of the same donor, we found that the expression levels of IGFPB5 transcripts were significantly higher in metastatic tissue than in primary tumor one (Fig. 8D). As shown in Figure 8E, the treatment with 1 and 10 μmol/L vorinostat for 24 h caused significant increase in IGFBP5 transcripts. Therefore, we determined whether the downregulation of $K_{Ca}3.1$ by HDAC inhibition is related to the expression levels of IGFBP5 in YMB-1 cells. As shown in Figure 8F, no significant changes in the expression levels of $K_{Ca}3.1$ transcripts were found in IGFBP5-overexpressing YMB-1 cells (Fig. 8C) when IGFBP5 transcription was over 10-fold increased by the transfection of pcDNA-IGFBP5 (not shown). These results indicated that $K_{Ca}3.1$ transcription was not regulated by REST and IGFBP5 in YMB-1 cells.

Expression of HDAC2, HDAC3, and $K_{Ca}3.1$ in human primary and metastatic breast tumor tissues

In various cancer types including breast cancer, the high level expression of $K_{Ca}3.1$ is associated with a high metastatic risk (Rabjerg et al. 2015). Since $K_{Ca}3.1$ levels increase with the progression of breast cancer, $K_{Ca}3.1$ may be useful for detecting malignancy grade during breast cancer progression (Haren et al. 2010). Using total RNAs from the primary breast tumor and corresponding metastatic breast tumor of the same donor, we found that the expression levels of $K_{Ca}3.1$ transcripts were lower in metastatic tissues than in primary tumor tissues (Fig. 9A). The expression levels of HDAC2 (Fig. 9B) and HDAC3 (Fig. 9C) transcripts were also significantly lower in metastatic tissues. These results suggest that the upregulation of $K_{Ca}3.1$ through HDAC2 and HDAC3 enhancements may be responsible for the pathogenesis of aggressive rather than metastatic breast cancer.

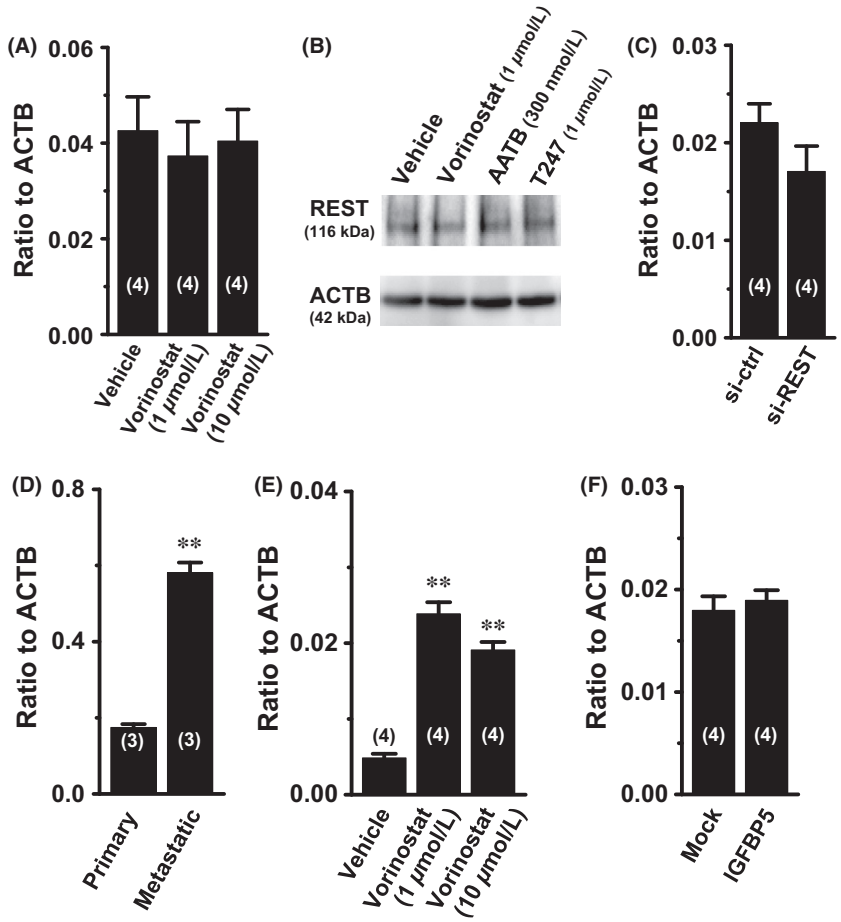

Figure 8. Effects of vorinostat on the expression levels of REST and IGFBP5 transcripts in YMB-1 cells, and effects of REST siRNA and IGFBP5 overexpression on the expression levels of $K_{Ca}3.1$ transcripts in YMB-1 cells. (A) Effects of vorinostat (1 and 10 μmol/L) (treatment for 24 h) on the expression levels of REST transcripts in YMB-1 cells. (B) Effects of vorinostat (1 μmol/L), AATB (300 nmol/L), and T247 (1 μmol/L) (treatment for 48 h) on the expression levels of REST proteins in YMB-1 cells. (C) Effects of REST siRNA on the expression levels of $K_{Ca}3.1$ transcripts in YMB-1 cells. (D) Comparison of the expression levels of IGFBP5 transcripts between human "primary" and "metastatic" breast tumors. (E) Effects of vorinostat (1 and 10 μmol/L) (treatment for 24 h) on the expression levels of IGFBP5 transcripts in YMB-1 cells. (F) Effects of overexpression of IGFBP5 on the expression levels of $K_{Ca}3.1$ transcripts in YMB-1 cells: mock, transfected with pcDNA3.1(+) alone; IGFBP5, transfected with pcDNA-IGFBP5. Expression levels were expressed as the ratio to ACTB. Results are expressed as means ± SEM. The numbers used for the experiments are shown in parentheses. The significance of differences among two and multiple groups was evaluated using the Student's *t*-test and Tukey's test. *, ** $P < 0.05$, 0.01 versus control siRNA (si-ctrl) (C), primary breast tumor (D), and vehicle control (E).

Discussion

The intermediate-conductance Ca^{2+}-activated K^+ channel, $K_{Ca}3.1$ has oncogenic potential and is a therapeutic target for $K_{Ca}3.1$-positive cancers such as renal (Rabjerg et al. 2015), lung (Bulk et al. 2015), hepatic, prostate cancers (Ohya et al. 2009), and glioblastoma (D'Alessandro et al. 2013). In breast cancer, $K_{Ca}3.1$ is associated with tumor progression and metastasis (Ouadid-Ahidouch et al. 2004; Faouzi et al. 2010; Haren et al. 2010). HDACis have potential as agents for the treatment of solid tumors including breast cancer (Slingerland et al. 2014), however, their effects on ion channel expression have not yet been elucidated in detailed. The main results of this study are as follows. (1) The clinically available pan-HDAC inhibitor, vorinostat significantly downregulated $K_{Ca}3.1$ transcription in the human breast cancer cell line YMB-1 (see Fig. 2). (2) The class I HDACs, HDAC2, and HDAC3 were responsible for the overexpression of $K_{Ca}3.1$ in YMB-1 cells (see Figs. 4 and 5). (3) HDAC2 and HDAC3 are also involved in the epigenetic regulation of $K_{Ca}3.1$ in the $K_{Ca}3.1$-expressing human prostate cancer cell line, PC-3 (see Fig. 6). We previously identified the dominant-negative splicing isoform of $K_{Ca}3.1$, $K_{Ca}3.1$B from mam-

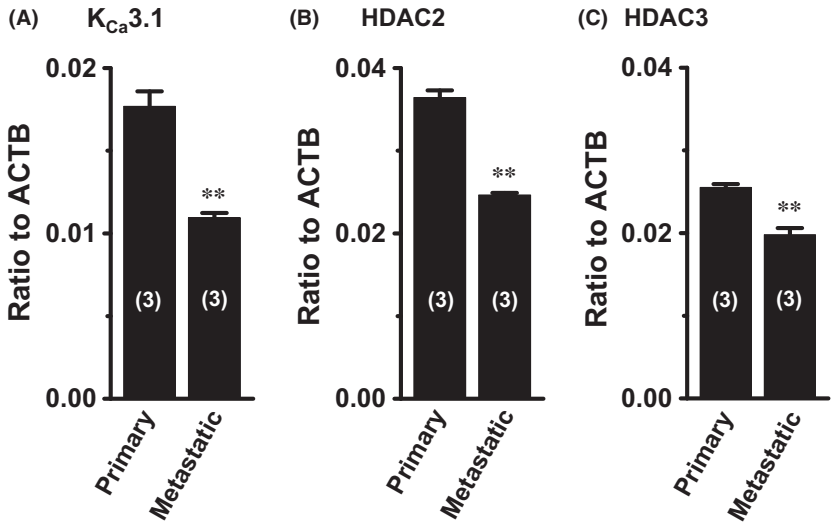

Figure 9. Comparison of the expression levels of $K_{Ca}3.1$, HDAC2, and HDAC3 transcripts between human primary and metastatic breast tumors. (A–D) Real-time PCR assay for $K_{Ca}3.1$ (A), HDAC2 (B), and HDAC3 (C) in human primary and metastatic breast tumors. Expression levels were expressed as the ratio to ACTB. Results are expressed as means ± SEM. The numbers used for the experiments are shown in parentheses. The significance of differences was evaluated using the Student's *t*-test. $^{**}P < 0.01$ versus primary breast tumors.

malian lymphoid cells (Ohya et al. 2011b). $K_{Ca}3.1B$ was expressed less abundantly in vehicle- and HDACis-treated YMB-1 cells (not shown).

HDAC2 and HDAC3 are strongly expressed in aggressive breast tumor subtypes (Müller et al. 2013). Their expression levels are also higher in HER2-positive breast tumor subtypes: 44% and 52% for HDAC2 and HDAC3, respectively. Consistent with this finding, HER2-positive YMB-1 and MDA-MB-453 cells strongly expressed HDAC1, 2, and 3 (Fig. S5A and B) (Matsuba et al. 2014). However, the expression levels of $K_{Ca}3.1$ transcripts markedly differed between these cell types (Fig. 1B). No correlation was detected between the expression levels of HER2 and $K_{Ca}3.1$ in human primary breast cancer tissues (Fig. S5C). Furthermore, HDAC1, HDAC2, and HDAC3 are highly expressed in human prostate cancer (Weichert et al. 2008). The expression levels of HDAC2 were previously reported to be high in patients with Gleason score 7 (Weichert et al. 2008). HDAC3 is also expected to become a potent therapeutic target for prostate cancer due to the consistently high rate of HDAC3 positivity (Weichert et al. 2008). We previously demonstrated that HDAC2 and HDAC3 were both predominatly expressed in $K_{Ca}3.1$-expressing PC-3 cells (Matsuba et al. 2014), while the expression level of $K_{Ca}3.1$ was found to be prominent in biopsy samples from patients with midgrade malignancy (Gleason score 5–6) (Ohya et al. 2009). These findings suggest that selective HDAC2 and 3 inhibitors have potential as therapeutic agents for $K_{Ca}3.1$-positive cancer.

HDACis upregulate tumor suppressor genes via histone hyperacetylation. It has been reported that the expression levels of REST and IGFBP5 is negatively correlated with that of $K_{Ca}3.1$ in proliferative cells including breast cancer calls (Cheong et al. 2005; Ohya et al. 2011a; Akkiprik et al. 2015). The transcription or protein degradation of REST is regulated by the treatment with HDACis in medulloblastoma (Taylor et al. 2012), however, this study showed no significant changes in the expression level of REST by the treatment with HDACis in YMB-1 cells (Fig. 8A and B). In addition, no significant changes in the expression level of $K_{Ca}3.1$ transcripts were detected by the siRNA-based blockade of REST expression in YMB-1 cells (Fig. 8C). These suggest that the downregulation of $K_{Ca}3.1$ by HDAC inhibition is not due to the upregulation of REST in YMB-1 cells. On the other hand, the expression level of IGFBP5 transcripts was significantly increased by vorinostat (Fig. 8D). In gastrointestinal stromal tumors, the expression level of the Ca^{2+}-activated Cl^- channel ANO1/TMEM16A was negatively correlated with that of IGFBP5 (Simon et al. 2013). This study showed no significant downregulation of $K_{Ca}3.1$ by the overexpression of IGFBP5 in YMB-1 cells (Fig. 8F). Of seven IGFBP subtypes (IGFBP1-7), IGFBP2 is predominatly expressed in YMB-1 cells, and no significant changes in $K_{Ca}3.1$ expression was caused by the overexpression of IGFBP2 (not shown). The destabilization of DNA methylation (hypermethylation or hypomethylation) in ion channels has been correlated with tumorigenesis and a poor prognosis (Ouadid-Ahidouch et al. 2015). Hypomethylation of the $K_{Ca}3.1$ promoter has recently been associated with the upregulation of $K_{Ca}3.1$ in aggressive nonsmall-cell lung cancer (Bulk et al. 2015), suggesting that the upregulation of

$K_{Ca}3.1$ may mediate the hypomethylation of its promoter gene in $K_{Ca}3.1$-expressing cancer cells. Further studies are needed in order to elucidate the mechanism underlying the epigenetic regulation of the $K_{Ca}3.1$ gene.

Similar to previous findings by Haren et al. (2010), this study showed that $K_{Ca}3.1$ was associated with the enhancement of breast cancer cell proliferation (Fig. 1). Large-conductance $K_{Ca}1.1$ and small-conductance $K_{Ca}2.3$ have been implicated in metastasis by facilitating breast cancer cell migration (Khaitan et al. 2009; Chantôme et al. 2013). Metalloproteinases 2 and 9 (MMP-2 and MMP-9) have been associated with breast cancer invasion (Jaafar et al. 2014; Vucemilo et al. 2014), and the reduction in MMP-2 may play a role in the suppressive effects of the $K_{Ca}3.1$ blocker on breast cancer migration and invasion (Zhang et al. 2015). Similar findings have been reported in glioma cells (D'Alessandro et al. 2013; Aroui et al. 2015). However, the expression levels of MMP-2 and MMP-9 were very low in YMB-1, and no significant changes were found in their expression by HDAC inhibition or pharmacological $K_{Ca}3.1$ blockade (not shown).

HDACis were primarily developed as antitumor agents, but are currently being explored for the treatment of neurodegenerative, immunological, metabolic, inflammatory, atopic, and cardiovascular disorders. Felice et al. (2015) recently showed that HDAC2 and HDAC3 isoforms were involved in chronic intestinal inflammation, and HDAC inhibition decreased disease responses in inflammatory bowel disease (IBD). HDACis including vorinostat ameliorate intestinal inflammation by inhibiting inflammatory cytokine production in the $CD4^+$ T cells of IBD model mice (Glauben et al. 2006). Recent studies including our previous study demonstrated that the upregulation of $K_{Ca}3.1$ in $CD4^+$ T cells was involved in the pathogenesis of IBD, and the pharmacological blockade of $K_{Ca}3.1$ elicited a significant decrease in IBD disease severity including intestinal inflammation (Di et al. 2010a; Ohya et al. 2014). Gillespie et al. (2012) also found that a selective HDAC3 inhibitor reduced the production of the proinflammatory cytokine, IL-6 in mononuclear cells from rheumatoid arthritis patients. The pharmacological and genetic inhibition of $K_{Ca}3.1$ was previously shown to suppress IL-6 levels in rheumatoid arthritis patients and allergic rhinitis model mice (Friebel et al. 2015; Lin et al. 2015). Furthermore, we reported the inhibition of IL-6 transcription by the pharmacological blockade of $K_{Ca}3.1$ in colonic inflammation in IBD model mice (Ohya et al. 2014). These suggest selective HDAC inhibition of HDAC2 and/or HDAC3 as a new therapeutic strategy to improve chronic inflammatory diseases.

In conclusion, this study demonstrated that the selective inhibition of HDAC2 and/or HDAC3 is a novel therapeutic strategy for drug development focused on $K_{Ca}3.1$-expressing cancer cells such as aggressive breast and prostate cancers. Moreover, HDAC2 and/or HDAC3 may become therapeutic targets for the treatment of chronic inflammatory and atopic disorders.

Acknowledgements

We thank to Anowara Khatun, Yurika Nakazono, Yuri Masuno, and Shinpei Ashino for their technical assistance. Medical English Service (Kyoto, Japan) reviewed the manuscript prior to submission.

Author Contributions

Participated in research design: S. Ohya, T. Suzuki, K. Muraki.

Conducted experiments: S. Ohya, S. Kanatsuka, N. Hatano, H. Kito, A. Matsui, M. Fujimoto, S. Matsuba, S. Niwa, P. Zhan.

Performed data analysis: S. Ohya, S. Kanatsuka, N. Hatano, H. Kito, A. Matsui, M. Fujimoto, S. Matsuba, S. Niwa, P. Zhan, T. Suzuki, K. Muraki.

Wrote or contributed to the writing of the manuscript: S. Ohya, S. Kanatsuka, N. Hatano.

Disclosures

None declared.

References

Akkiprik M, Peker İ, Özmen T, Amuran GG, Güllüoğlu BM, Kaya H, et al. (2015). Identification of differentially expressed IGFBP5-related genes in breast cancer tumor tissues using cDNA microarray experiments. Genes (Basel) 6: 1201–1214.

Aroui S, Najlaoui F, Chtourou Y, Meunier AC, Laajimi A, Kenani A, et al. (In Press). Naringin inhibits the invasion and migration of human glioblastoma cell via downregulation of MMP-2 and MMP-9 expression and inactivation of p38 signaling pathway. Tumour Biol doi:10.1007/s13277-015-4230-4

Attwood PV, Wieland T (2015). Nucleoside diphosphate kinase as protein histidine kinase. Naunyn Schmiedebergs Arch Pharmacol 388: 153–160.

Bergmeier W, Weidinger C, Zee I, Feske S (2013). Emerging roles of store-operated Ca^{2+} entry through STIM and ORAI proteins in immunity, hemostasis and cancer. Channels (Austin) 7: 379–391.

Bose P, Dai Y, Grant S (2014). Histone deacetylase inhibitor (HDACI) mechanisms of action: emerging insights. Pharmacolgical Ther 143: 323–336.

Bulk E, Ay AS, Hammadi M, Ouadid-Ahidouch H, Schehaas S, Hascher A, et al. (2015). Epigenetic dysregulation of $K_{Ca}3.1$

channels induces poor prognosis in lung cancer. Int J Cancer 137: 1306–1307.

Cahalan MD, Chandy KG (2009). The functional network of ion channels in T lymphocytes. Immunol Rev 231: 59–87.

Chantôme A, Potier-Cartereau M, Clarysse L, Fromont G, Marionneau-Lambot S, Guéguinou M, et al. (2013). Pivotal role of the lipid Raft SK3-Orai1 complex in human cancer cell migration and bone metastases. Cancer Res 73: 4852–4861.

Cheong A, Bingham AJ, Li J, Kumar B, Sukumar P, Munsch C, et al. (2005). Downregulated REST transcription factor is a switch enabling critical potassium channel expression and cell proliferation. Mol Cell 20: 45–52.

Comes N, Serrano-Albarrás A, Capera J, Serrano-Novillo C, Condom E, Cajal S, et al. (2015). Involvement of potassium channels in the progression of cancer to more malignant phenotype. Biochim Biophys Acta 1848: 2477–2492.

D'Alessandro G, Catalano M, Sciaccaluga M, Chece G, Cipriani R, Rosito M, et al., (2013) $K_{Ca}3.1$ channels are involved in the infiltrative behavior of glioblastoma in vivo. Cell Death Dis 4: e773.

Di L, Srivastava S, Zhdanova O, Ding Y, Li Z, Wulff H, et al. (2010a). Inhibition of the K^+ channel $K_{Ca}3.1$ ameliorates T cell-mediated colitis. Proc Natl Acad Sci USA 10: 1541–1546.

Di L, Srivastava S, Zhdanova O, Sun Y, Li Z, Skolnik EY (2010b). Nucleoside diphosphate kinase B knock-out mice have impaired activation of the K^+ channel $K_{Ca}3.1$, resulting in defective T cell activation. J Biol Chem 285: 38765–38771.

Faouzi M, Chopin V, Ahidouch A, Ouadid-Ahidouch H (2010). Intermediate Ca^{2+}-sensitive K^+ channels are necessary for prolactin-induced proliferation in breast cancer cells. J Membrane Biol 234: 47–56.

Felice C, Lewis A, Armuzzi A, Lindsay JO, Silver A (2015). Review article: selective histone deacetylase isoforms as potential therapeutic targets in inflammatory bowel diseases. Aliment Pharmacol Ther 41: 26–38.

Feske S, Wulff H, Skolnik EY (2015). Ion channels in innate and adaptive immunity. Annu Rev Immunol 33: 291–353.

Friebel K, Schonherr R, Kinne RW, Kunisch E (2015). Functional role of the $K_{Ca}3.1$ potassium channel in synovial fibroblasts from rheumatoid arthritis patients. J Cell Physiol 230: 1677–1688.

Ghoussaini M, Edwards SL, Michailidou K, Nord S, Cowper-Sal Lari R, Desai K, et al. (2014). Evidence that breast cancer risk at the 2q35 locus is mediated through IGFBP5 regulation. Nat Commun 4: 4999.

Gillespie J, Savie S, Wong C, Hempshell A, Inman M, Emery P, et al. (2012). Histone deacetylases are dysregulated in rheumatoid arthritis and a novel histone deacetylase 3-selective inhibitor reduces inerleukin-6 production by peripheral blood mononuclear cells from rheumatoid arthritis patients. Arthritis Rheum 64: 418–422.

Glauben R, Batra A, Fedke I, Zeitz M, Lehr HA, Mascagni P, et al. (2006). Histone hyperacetylation is associated with amelioration of experimental colitis in mice. J Immunol 176: 5015–5022.

Haren N, Khorsi H, Faouzi M, Ahidouch A, Sevestre H, Ouadid-Ahidouch H (2010). Intermediate conductance Ca^{2+} activated K^+ channels are expressed and functional in breast adenocarcinomas: correlation with tumour grade and metastasis status. Histol Histopathol 25: 1247–1255.

Huang X, Jan LY (2014). Targeting potassium channels in cancer. J Cell Biol 206: 151–162.

Itoh Y, Suzuki T, Kouketsu A, Suzuki N, Maeda S, Yoshida M, et al. (2007). Design, synthesis, structure-selectivity relationship, and effect on human cancer calls of a novel series of histone deacetylase 6-selective inhibitors. J Med Chem 50: 5425–5438.

Jaafar H, Sharif SE, Murtey MD (2014). Pattern of collagen fibers and localization of matrix metalloproteinase 2 and 9 during breast cancer invasion. Tumori 100: e204–e211.

Khaitan D, Sankpal UT, Weksler B, Meister EA, Romero IA, Couraud PO, et al. (2009). Role of KCNMA1 gene in breast cancer invasion and metastasis to brain. BMC Cancer 9: 258.

Lin H, Zheng C, Li J, Yang C, Hu L (2015) Lentiviral shRNA against $K_{Ca}3.1$ inhibits allergic response in allergic rhinitis and suppresses mast cell activity via PI3K/AKT signaling pathway. Sci Rep 5: 13127.

Matsuba S, Niwa S, Muraki K, Kanatsuka S, Nakazono Y, Hatano N, et al. (2014). Downregulation of Ca^{2+}-activated Cl^- channel TMEM16A by the inhibition of histone deacetylase in TMEM16A-expressing cancer cells. J Pharmacol Exp Ther 351: 510–518.

Methot JL, Chalravarty PK, Chenard M, Close J, Cruz JC, Dahlberg WK, et al. (2008). Exploration of the internal cavity of histone deacetylase (HDAC) with selective HDAC1/HDAC2 inhibitors (SHI-1:2). Bioorg Med Chem Lett 18: 973–978.

Michailidou K, Hall P, Gonzalez-Neira A, Ghoussaini M, Dennis J, Milne RL, et al. (2013). Large-scale genotyping identifies 41 new loci associated with breast cancer risk. Nat Genet 45: 353–361.

Müller BM, Jana L, Kasajima A, Lehmann A, Prinzler J, Budczies J, et al. (2013). Differential expression of histone deacetylases HDAC1, 2 and 3 in human breast cancer – overexpression of HDAC2 and HDAC3 is associated with clinicopathological indicators of disease progression. BMC Cancer 13: 215.

Munster PN, Thurn KT, Thomas S, Raha P, Lacevic M, Miller A, et al. (2011). A phase II study of the histone deacetylase

inhibitor vorinostat combined with tamoxifen for the treatment of patients with hormone therapy-resistant breast cancer. Br J Cancer 104: 1828–1835.

Ohya S, Kimura K, Niwa S, Ohno A, Kojima Y, Sasaki S, et al. (2009). Malignancy grade-dependent expression of K^+-channel subtypes in human prostate cancer. J Pharmacol Sci 109: 148–151.

Ohya S, Niwa S, Kojima Y, Sasaki S, Sakuragi M, Kohri K, et al. (2011a). Intermediate-conductance Ca^{2+}-activated K^+ channel, $K_{Ca}3.1$, as a novel therapeutic target for benign prostatic hyperplasia. J Pharmacol Exp Ther 338: 528–536.

Ohya S, Niwa S, Yanagi A, Fukuyo Y, Yamamura H, Imaizumi Y (2011b). Involvement of dominant-negative spliced variants of the intermediate conductance Ca^{2+}-activated K^+ channel, $K_{Ca}3.1$, in immune function of lymphoid cells. J Biol Chem 286: 16940–16952.

Ohya S, Fukuyo Y, Kito H, Shibaoka R, Matsui M, Niguma H, et al. (2014). Upregulation of $K_{Ca}3.1$ K^+ channel in mesenteric lymph node $CD4^+$ T lymphocytes from a mouse model of dextran sodium sulfate-induced inflammatory bowel disease. Am J Physiol Gastrointest Liver Physiol 306: G873–G885.

Ouadid-Ahidouch H, Ahidouch A (2013). K^+ channels and cell cycle progression in tumor cells. Front Physiol 4: 220.

Ouadid-Ahidouch H, Roudbaraki M, Delcourt P, Ahidouch A, Joury N, Prevarskaya N (2004). Functional and molecular identification of intermediate-conductance Ca^{2+}-activated K^+ channels in breast cancer cells; association with cell cycle progression. Am J Physiol Cell Physiol 287: C125–C134.

Ouadid-Ahidouch H, Rodat-Despoix L, Matifat F, Morin G, Ahidouch A (2015). DNA methylation of channel-related genes in cancers. Biochim Biophys Acta 1848: 2621–2628.

Pardo LA, Stühmer W (2014). The roles of K^+ channels in cancer. Nat Rev Cancer 14: 39–48.

Rabjerg M, Oliván-Viguera A, Hansen LK, Jensen L, Sevelsted-Møller L, Walter S, et al. (2015). High expression of $K_{Ca}3.1$ in patients with clear cell renal carcinoma predicts high metastatic risk and poor survival. PLoS ONE 10: e1022992.

Ramaswamy B, Fiskus W, Cohen B, Pellegrino C, Hershman DL, Chung E, et al. (2012). Phase I-II study of vorinostat plus paclitazel and bevacizumab in metastatic breast cancer: evidence for vorinostat-induced tubulin acetylation and Hsp90 inhibition in vivo. Breast Cancer Res Treat 132: 1063–1072.

Seo J, Min SK, Park HR, Kim DH, Kwon MJ, Kim LS, et al. (2014). Expression of histone deacetylases HDAC1, HDAC2, HDAC3, and HDAC6 in invasive ductal carcinomas of the breast. J Breast Cancer 17: 323–331.

Simon S, Grabellus F, Ferrera L, Galietta L, Schwindenhammer B, Mühlenberg T, et al. (2013). DOG1 regulates growth and IGFBP5 in gastrointestinal stromal tumors. Cancer Res 73: 3661–3679.

Slingerland M, Hj Guchelaar, Gelderblom H (2014). Histone deacetylase inhibitors: an overview of the clinical studies in solid tumors. Anticancer Drugs 25: 140–149.

Srivastava S, Ko K, Choudhury P, Li Z, Johnson AK, Nadkauni V, et al. (2006). Phosphatidylinositol-3 phosphatase myotubularin-related protein 6 negatively regulates CD4 T cells. Mol Cell Biol 26: 5595–5602.

Srivastava S, Zhdanova O, Di L, Li Z, Albaqumi M, Wulff H, et al. (2008). Protein histidine phosphatase 1 negatively regulates CD4 T cells by inhibiting the K^+ channel $K_{Ca}3.1$. Proc Natl Acad Sci USA 105: 14442–14446.

Srivastava S, Di L, Zhdanova O, Li Z, Vardhana S, Wan Q, et al. (2009). The class II phosphatidylinositol 3 kinase C2β is required for the activation of the K^+ channel $K_{Ca}3.1$ and $CD4^+$ T-cells. Mol Biol Cell 20: 3783–3791.

Suzuki T, Kasuya Y, Itoh Y, Ota Y, Zhan P, Asamitsu K, et al. (2013). Identification of highly selective and potent histone deacetylase 3 inhibitors using click chemistry-based combinatorial fragment assembly. PLoS ONE 8: e68669.

Suzuki T, Khan MN, Sawada H, Imai E, Itoh Y, Yamatsuta K, et al. (2012). Design, synthesis, and biological activity of a novel series of human sirtuin-2-selective inhibitors. J Med Chem 55: 5760–5773.

Taylor P, Fangusaro J, Rajaram V, Goldman S, Helenowski IB, MacDonald T, et al. (2012). REST is a novel prognostic factor and therapeutic target for medulloblastoma. Mol Cancer Ther 11: 1713–1723.

Vucemilo T, Skoko M, Sarcević B, Puljiz M, Alvir I, Turudić TP, et al. (2014). The level of serum pro-matrix metalloproteinase-2 as a prognostic factor in patients with invasive ductal breast cancer. Coll Antropol 38: 135–140.

Wang H, Arun BK, Wang H, Fuller GN, Zhang W, Middleton LP, et al. (2008). IGFBP2 and IGFBP5 overexpression correlates with the lymph node metastasis in T1 breast carcinomas. Breast J 14: 261–267.

Weichert W, Roske A, Gekeler V, Beckers T, Stephan C, Jung K, et al. (2008). Histone deacetylases 1, 2 and 3 are highly expressed in prostate cancer and HDAC2 expression is associated with shorter PSA relapse time after radical prostatectomy. Br J Cancer 98: 604–610.

West AC, Johnstone RW (2014). New and emerging HDAC inhibitors for cancer treatment. J Clin Invest 124: 30–39.

Wulff H, Castle NA (2010). Therapeutic potential of $K_{Ca}3.1$ blockers: an overview of recent advances, and promising trends. Expert Rev Clin Pharmacol 3: 385–396.

Zhang Y, Feng Y, Chen L, Zhu J (2015). Effects of intermediate-conductance Ca^{2+}-activated K^+ channels on human endometrial carcinoma cells. Cell Biochem Biophys 72: 515–525.

Supporting Information

Additional Supporting Information may be found online in the supporting information tab for this article:

Figure S1. Expression levels of PRL receptor (PRLR) transcripts in human breast cancer cell lines, and effects of chemotherapy agents (paclitaxel and bafilomycin-A) and the SIRT1/2 inhibitor, NCO-04. (A) Expression levels of PRLR transcripts in YMB-1, MCF-8, Hs578T, BT549, and MDA-MB-453 cells were determined. (B) Effects of paclitaxel (100 nmol/L) and bafilomycin-A (10 nmol/L) on the expression levels of $K_{Ca}3.1$ transcripts in YMB-1 cells. (C) Expression levels of class III HDACs, sirtuin subtype (SIRT1-7) transcripts in YMB-1, (D) Effects of NCO-04 on the expression levels of $K_{Ca}3.1$ transcripts in YMB-1 cells. Expression levels were expressed as a ratio to ACTB. Results are expressed as means ± SEM (n = 3–4). The following gene-specific PCR primers of human origin were used: PRLR (NM_000949, 1904-2025), 122 bp; SIRT 1 (NM_012238, 2004-2124), 121 bp; SIRT2 (NM_012237, 977-1097), 121 bp; SIRT3 (NM_012239, 704-824), 121 bp; SIRT4 (NM_012240, 888-1008), 121 bp; SIRT5 (NM_012241, 1071-1191), 121 bp; SIRT6 (NM_016539, 188-322), 135 bp; SIRT7 (NM_016538, 968-1088), 121 bp.

Figure S2. Expression levels of various types of K^+ channel transcripts in YMB-1 cells. (A) voltage-gated Kv1 subtypes. (B) voltage-gated Kv2, Kv3, and Kv4 subtypes. (C) Kv10, 11, and 12 subtypes. (D) Kv7 subtypes. (E) K_{2P} subtypes. (F) K_{Ca} subtypes and $K_{ir}2.1$. Expression levels were expressed as a ratio to ACTB. Results are expressed as means ± SEM (n = 4). The following gene-specific PCR primers of human origin were used for real-time PCR: Kv1.1 (GenBank accession number: NM_000217, 967-1072), 106 bp; Kv1.2 (NM_004974, 94-194), 101 bp; Kv1.3 (XM_084080, 1411-1517), 107 bp; Kv1.4 (NM_002233, 1145-1245), 101 bp; Kv1.5 (XM_006988, 1968-2092), 125 bp; Kv1.6 (XM_018513, 1401-1504), 104 bp; Kv1.7 (AJ310479, 1456-1598), 143 bp; Kv2.1 (NM_004975, 950-1050), 101 bp; Kv2.2 (NM_004770, 221-321), 101 bp; Kv3.1 (NM_004976, 647-747), 101 bp; Kv3.2 (AF268897, 1418-1519), 102 bp; Kv3.3 (AF055989, 2649-2771), 123 bp; Kv3.4 (NM_004978, 839-946), 108 bp; Kv4.1 (NM_004979, 1494-1598), 105 bp; Kv4.2 (NM_012281, 2275-2384), 110 bp; Kv4.3 (NM_004980, 1707-1807), 101 bp; Kv7.1 (NM_000218, 1556-1656), =101 bp; Kv7.2 (NM_004518, 536-664), 129 bp; Kv7.3 (NM_004519, 1958-2058), 101 bp; Kv7.4 (NM_004700, 1741-1841), 101 bp; Kv7.5 (NM_019842, 341-443), 103 bp; Kv10.1 (NM_002238, 1640-1761), 122 bp; Kv10.2 (NM_139318, 2109-2209), 101 bp; Kv11.1 (NM_000238, 2718-2823), 106 bp; Kv11.2 (NM_030779, 32-172), 141 bp; Kv11.3 (NM_033272, 3558-3658), 101 bp; Kv12.1 (NM_144633, 688-798), 111 bp, Kv12.2 (XM_035483, 1137-1237), 101 bp; Kv12.3 (NM_012285, 1340-1444), 105 bp; $K_{2P}1.1$ (NM_002245, 948-1048), 101 bp; $K_{2P}2.1$ (NM_014217, 849-949), 101 bp; $K_{2P}3.1$ (NM_002246, 622-744), 123 bp; $K_{2P}4.1$ (NM_016611, 413-538), 126 bp; $K_{2P}5.1$ (EU978936, 577-697), 121 bp; $K_{2P}6.1$ (NM_004823, 1136-1252), 117 bp; $K_{2P}7.1$ (NM_033347, 827-966), 140 bp; $K_{2P}9.1$ (NM_016601, 1025-1146), 122 bp; $K_{2P}10.1$ (NM_021161, 702-802), 101 bp; $K_{2P}12.1$ (NM_022055, 382-497), 116 bp; $K_{2P}13.1$ (NM_022054, 1587-1722), 136 bp; $K_{2P}15.1$ (NM_022358, 1094-1206), 113 bp; $K_{2P}16.1$ (NM_001135105, 805-925), 121 bp; $K_{2P}17.1$ (NM_031460, 444-563), 120 bp; $K_{2P}18.1$ (NM_181840, 849-969), 121 bp; $K_{Ca}1.1$ (NM_001014797, 679-798), 120 bp; $K_{Ca}2.1$ (NM_002248, 649-764), 116 bp; $K_{Ca}2.2$ (NM_021614, 1492-1612), 121 bp: $K_{Ca}2.3$ (NM_002249, 2042-2146), 105 bp; $K_{Ca}4.1$ (NM_020822, 1719-1845), 127 bp; $K_{Ca}4.2$ (NM_198503, 1826-1946), 121 bp; $K_{ir}2.1$ (NM_000891, 765-865), 101 bp.

Figure S3. Measurement of 1 μmol/L TRAM-34-sensitive currents and store-operated Ca^{2+} entry (SOCE) in YMB-1 cells and effects of 1 μmol/L TRAM-34 on relative AUC of $[Ca^{2+}]_i$ in HDACis-treated YMB-1 cells. (A and B) schematic diagrams of the analytical methods to calculate 1 μmol/L TRAM-34-sensitive currents (A) and relative AUC of $[Ca^{2+}]_i$ (B) (see "Materials and Methods"). 0 Ca^{2+}: 0 mmol/L Ca^{2+}, 2.2 Ca^{2+}: 2.2 mmol/L Ca^{2+}, TG: 1 μmol/L thapsigargin, AUC: area under the curve. (C and D) Effects of TRAM-34 (1 μmol/L) on relative AUC of $[Ca^{2+}]_i$ SOCE in 300 nmol/L AATB- and 1 μmol/L T247-treated YMB-1 cells for 30–48 h. Results are expressed as means ± SEM. Numbers used for the experiments are shown in parentheses.

Figure S4. Transcriptional expression levels of the regulatory molecules of $K_{Ca}3.1$ in human breast normal and tumor tissues. Real-time PCR assay for PI3K-C2B (A), PHPT1 (B), and MTMR6 (C). The expression levels were expressed as the ratio to ACTB. The results are expressed as the means ± SEM (n = 3 for each). The following gene-specific PCR primers of human origin were used: PI3K-C2B (NM_002646, 4052-4172), 121 bp; PHPT1 (NM_001135861, 783-903), 121 bp; MTMR6 (NM_004685, 1476-1607), 132 bp.

Figure S5. Expression levels of (A) HER2 transcripts in human breast cancer cell lines (YMB-1, MCF-7, Hs578T, BT549 and MDA-MB-453) (n = 3), (B) HDAC1, HDAC2, HDAC3, and HDAC6 transcripts in MDA-MB-453 cells (n = 4), and (C) $K_{Ca}3.1$ and HER2 transcripts in human primary breast tumor tissues (n = 5). Expression levels were expressed as a ratio to ACTB. Results are expressed as means ± SEM. The following gene-specific PCR primers of human origin were used: HER2 (NM_004448, 1440-1559), 120 bp; HDAC1 (NM_004964, 708-824), 117 bp; HDAC6 (NM_006044, 3517-3637), 121 bp.